Available online at www.sciencedirect.com
SCIENCE DIRECT®
Journal of Magnetic Resonance 175 (2005) 73–78
JMR Journal of Magnetic Resonance
www.elsevier.com/locate/jmr

Non-destructive observation of electrically detected magnetic resonance in bulk material using AC bias

Toshiyuki Sato [a], Hidekatsu Yokoyama [b,*], Hiroaki Ohya [b]

[a] Yamagata Research Institute of Technology, Yamagata 990-2473, Japan
[b] Institute for Life Support Technology, Yamagata Promotion Organization for Industrial Technology, Yamagata 990-2473, Japan

Received 20 January 2005; revised 25 March 2005
Available online 27 April 2005

Abstract

DC bias is normally found in conventional measurements of electrically detected magnetic resonance (EDMR). Usually, electrodes are formed on the sample surface to make ohmic contacts for detecting changes in the electrical characteristics of the sample material. Thus, destructive procedures are required to detect the EDMR signal of bulk material with such methods. An AC bias detection technique was developed to allow the non-destructive EDMR measurement of bulk materials. An AC bridge circuit was constructed to detect the change in impedance of the sample, which when changed by ESR, an unbalanced AC voltage can be detected. By detecting this AC bias, it is possible to cancel the effects, such as Shottky barriers, that disturb the ohmic contact between the electrodes and a sample material. Further, the AC bias current penetrates the thin surface layer of a sample such as silicon oxide, which normally obstructs a DC current. This method was utilized using conductive rubber contacts for non-destructive EDMR measurements of part of a silicon wafer. EDMR spectra observed were the same as those obtained by the conventional method of using DC bias detection.
© 2005 Elsevier Inc. All rights reserved.

Keywords: EDMR; AC bias; Bulk material; UHF; Silicon wafer

1. Introduction

Electrically detected magnetic resonance (EDMR) spectroscopy [1,2], also cited as spin-dependent recombination (SDR), is a method to observe magnetic resonance by detecting the change in the electrical characteristics of a sample. Using this method, highly sensitive and selective detection of paramagnetic recombination centers formed by lattice defects or impurities in a sample can be achieved. The technique has been applied to investigate items such as silicon diodes, metal-oxide-semiconductor field effect transistors (MOSFETs), and amorphous silicon. EDMR has also been shown applicable to III–V compound semiconductors such as GaAs and GaN devices [3,4].

The enhancement of EDMR sensitivity, compared to conventional ESR detection, has been explained by using an electron–hole pair model [5,6], which also predicts that the relationship between EMDR signal intensity and static magnetic field strength is not linear. EDMR sensitivity is reported as constant in a high field (>100 mT), but decreased in a lower field (<4 mT) [7–10]. Recently, in both experiments and theory, the relationship between EDMR signal intensity and magnetic fields of 10–32 mT, a range that bridges the gap between high- and low-field regions, has been clarified [11,12]. For lower magnetic fields (i.e., at longer microwave wavelengths), a larger sample space is available and the skin effect caused by the conductivity of the sample is reduced. We have built and evaluated an EDMR instrument operating at 900 MHz [13], wherein an ESR resonator with a 44 mm diameter was available; and the EDMR signal from silicon was reduced to only

* Corresponding author. Fax: +81 52 736 7304.
E-mail address: yokohide@ni.aist.go.jp (H. Yokoyama).

1090-7807/$ - see front matter © 2005 Elsevier Inc. All rights reserved.
doi:10.1016/j.jmr.2005.03.018

3/4 of the saturation level in a high field. We also developed an EDMR imaging system operating at 900 MHz under field gradients; with which an EDMR image of a 20 mm square silicon plate was obtained. The EDMR signal was not obtained from the interface between the semiconductor and the metal electrode, but originated from the silicon plate itself [14,15].

To observe EDMR of a bulk material, electrodes are formed on the surface of the sample to make ohmic contact. In this way, the change of electrical characteristics caused by ESR can be observed by applying a DC current through the sample. The material for the electrodes must be carefully selected to avoid formation of a Schottky barrier. The surface of the material can sometimes be oxidized or polluted; thus, preventing a good contact between the sample material and the electrodes; making it necessary to remove the surface layer and form the electrodes on the sample material. Ordinarily these electrodes are formed by evaporating or spattering a metal; therefore, in conventional EDMR studies, the sample will be damaged. When an EDMR spectrum is obtained from a sample material without imaging, it is difficult to determine whether the signal has been obtained from the bulk area or the interface between the electrodes and the sample.

In this study, an AC bias detection technique was developed to enable non-destructive EDMR measurements of bulk materials. When employed, this method can cancel the effects that disturb ohmic contact between the electrodes and a sample. The AC bias current can penetrate the thin surface layer (such as a SiO_2 layer of silicon) that will obstruct a DC current; so by utilizing AC bias detection, non-destructive EDMR measurements become possible.

2. Experiment

2.1. EDMR spectrometer

A block diagram of an EDMR spectrometer, fabricated to operate at an ESR frequency of 900 MHz, is shown in Fig. 1. The static magnetic field ($\mathbf{B}_0$) was set at 31 mT, and the sweep width and time were set at 5 mT and 30 s, respectively. The magnetic field was modulated at 362 Hz by a pair of modulation coils for lock-in detection. The modulation signal was generated by an oscillator (AFG 320, Sony Tektronix, Japan; frequency range, 10 mHz to 16 MHz; dual channel output). The modulation coils were driven by a power amplifier (4020, NF, Japan; gain, 46 dB). To improve the signal-to-noise ratio (SNR), 30 field sweeps were averaged to obtain one spectrum. A synthesized signal generator (MG3633A, Anritsu, Japan; frequency range, 10 kHz–2700 MHz) was used as a microwave source. The microwave power was amplified to 1 W by a power amplifier

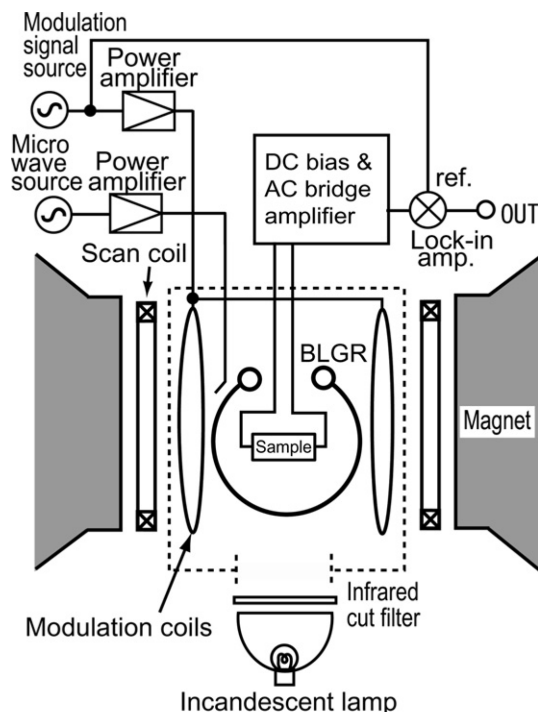

Fig. 1. Block diagram of an AC/DC bias EDMR spectrometer.

(A1000-1050, R&K, Japan; gain, 46 dB; output impedance, 50 Ω; bandwidth, 200 MHz–1 GHz; and maximum power, 50 W). A bridged shield loop-gap resonator (BLGR) was used so that the microwave field ($\mathbf{B}_1$) would be efficiently and uniformly applied to the sample [16,17]. The resonant frequency and the unloaded Q of the BLGR were 890 MHz and 510, respectively. The inner diameter and the axial length of the BLGR were 43 and 10 mm, respectively. A magnetic coupling loop, in which the coupling could be adjusted by moving the loop along the axial direction, was used. The BLGR was covered with a shield case so that radiation of microwave power was prevented and noise penetration inhibited. The sample was illuminated by a halogen incandescent lamp and the infrared part of the spectrum was reduced by a glass filter (KG-1; Edmund Optics, Barrington, NJ; cut off, 700 nm).

A block diagram of the detection circuit using AC bias is shown in Fig. 2. To generate a sine wave voltage, the oscillator (AFG 320) was used as an AC signal source; an AC voltage of 0.6 V peak-to-peak being applied to the AC bridge circuit at an AC bias frequency. The AC bridge consisted of two resistors, the sample, and variable resistor and capacitor sub-circuits. The variable resistor sub-circuit was constructed of five fixed resistors (10, 20, 40, 80, and 160 kΩ) and a 10 kΩ variable resistor connected in serial. All of the fixed resistors could be shorted selectively by relays to obtain a relay from 10 to 320 kΩ in 10 kΩ steps. The 10 kΩ variable resistor was used for fine tuning. The variable capacitor sub-circuit was constructed of four fixed mica capacitors

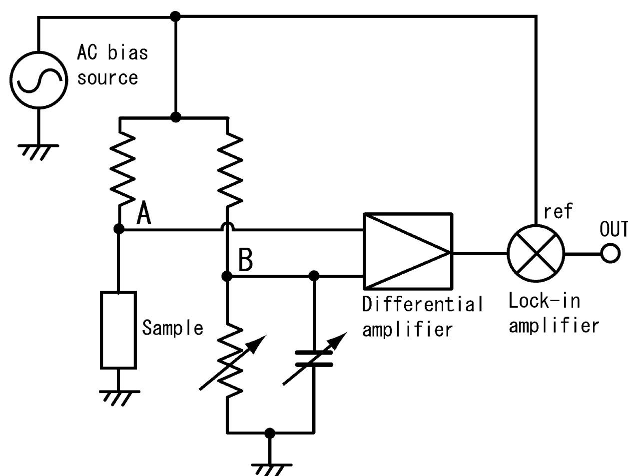

Fig. 2. Block diagram of the detection circuit using AC bias.

(100, 200, 400, and 800 pF) and a variable capacitor (200 pF; air gap) connected in parallel. All of the fixed capacitors could be connected selectively by relays to obtain 100–1600 pF of capacitance in 100 pF steps. The 200 pF variable capacitor was used for fine tuning. A resistor and capacitor in parallel at a constant frequency can be substituted for the impedance of the sample, so that the bridge can be balanced by tuning the resistor and capacitor in the sub-circuits. When balanced, the voltage between A and B in Fig. 2 is zero. When the impedance of the sample is changed by ESR, an AC voltage differential appears between A and B. The AC signal is amplified by a differential amplifier (gain, 32 dB; bandwidth 200 kHz, as constructed in our laboratory) and converted at the AC frequency into a DC voltage by a lock-in amplifier (LI5640, NF, Japan; frequency range, 1 mHz to 100 kHz; minimum time constant, 10 μs).

To compare a conventional method with our AC bias detection, a DC current source and a high input-impedance preamplifier were used to detect the change of conductance of the sample [13]. The sample was biased at a constant DC current of 10 μA, and the AC and DC detection circuits were alternately switched without altering any other conditions.

The change in the electrical characteristics of the sample due to the ESR irradiation was synchronized with the field modulation frequency (362 Hz). When the magnetic field was swept, another lock-in amplifier (5210, PARC, Princeton, NJ; frequency range 0.5 Hz to 120 kHz) detected the field modulation frequency and the differential EDMR spectrum was recorded. Instrumentation was controlled by a personal computer (PC9821Xa13, NEC, Japan) via a D/A converter (DAJ98, Canopus, Japan) and spectral data were collected via an A/D converter (ADJ98, Canopus), again using the personal computer.

2.2. Sample holder

The EDMR of the sample was measured using the sample holder shown in Fig. 3. Two Teflon holders (diameter, 33.4 mm; thickness, 5 mm) were placed in a quartz glass tube (inner diameter, 33.5 mm; outer diameter, 38 mm) to sandwich the sample. Two polycarbonate bolts and nuts were used to fasten the holders together. A 16 × 9 mm window was located at the center of one holder for illumination. A pair of gold plated copper contacts was attached to the other holder and a pair of conductive rubber pads (S60; Kinugawa Gomu Industry, Japan; volume resistance, 1 Ω cm; thickness, 0.5 mm) was attached to the copper contacts to augment conductance between the sample and the copper contacts. A pair of copper wires (0.26 mm in diameter), soldered to the copper contacts, conducted the electrical signal to a semirigid coaxial cable. The wire size was small enough to not disturb $\mathbf{B}_1$ in the BLGR. The coaxial cable was connected to the detection circuits. A Styrofoam spacer (diameter, 33.5 mm; thickness 48 mm), glued to the Teflon holder, held the pair of wires and the semirigid coaxial cable. The spacer was also used to keep the Teflon holders perpendicular to the axial direction of the quartz glass tube, which was set at the center of the BLGR.

2.3. Sample

An (100) oriented slice of an n-type 3.5-in. silicon wafer (thickness, 0.5 mm; resistance, 5 kΩ cm) was used as the sample material. An aqueous solution of 66% H_2SO_4 and 11% H_2O_2 was used to clean the surface on the sample. An aqueous solution of 1% HF was used to etch off the SiO_2 layer at the sample surface. Metal electrodes were formed by depositing chromium (see Fig. 4A) to a thickness of 400 Å onto the surface of the polished silicon. Then gold was deposited onto the chromium layer to a thickness of 2000 Å. The sample was cut into a rectangular plate (width, 8 mm; length, 19 mm). Left sitting in a room at ambient temperature, the surface of the sample was spontaneously re-oxidized.

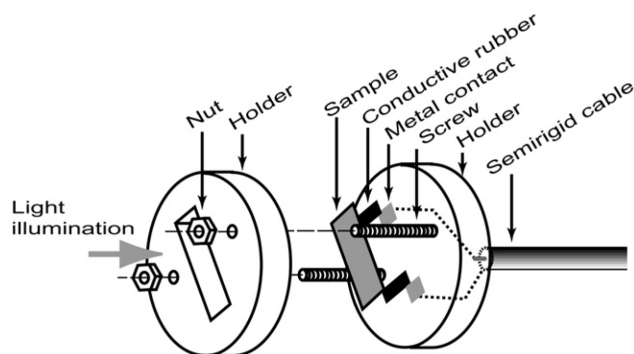

Fig. 3. Schema of a sample holder for AC bias EDMR measurement.

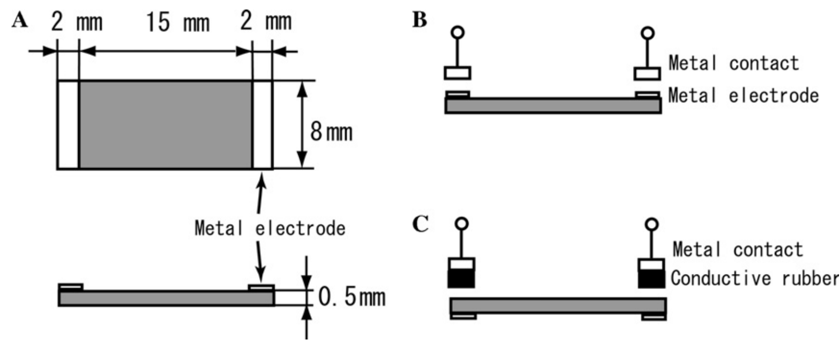

Fig. 4. Schema of a sample and contacts. Sample and formed metal electrode sizes are shown in (A). The change in impedance was measured with (B) or without (C) metal electrodes on the sample surface.

3. Results and discussion

3.1. Impedance of the sample

The impedance of the sample (including the holder) measured with an impedance analyzer (4192A; frequency, 100 Hz to 13 MHz; Hewlett–Packard, Palo Alto, CA) is plotted in Fig. 6. The sample was set in the holder and illuminated to excite excessive carriers. The conductive rubber was attached on the surface of the sample where the metal electrodes were not formed as shown in Fig. 4C. The impedance of the sample was expressed as a parallel connection of real and imaginary components at the AC bias frequencies, as shown in Fig. 5C. The solid circles and open squares on the plots show the real and imaginary components, respectively, of the sample. An equivalent circuit for the sample is shown in Fig. 5A. R_{oxide} and R_{sample} correspond to the resistance of the oxidized layer and the sample material, respectively; C_{holder} to the total capacitance of the holder and the cable; and C_{oxide} to the capacitance of the oxide layer of the sample. The oxide layer of the silicon is basically an insulator; however, it has dielectric loss and leakage caused by local thinness or defects. The oxide layer can therefore be expressed as a resistor and capacitor connected in parallel. The impedances of the oxide layers on both sides of the sample can be combined into R_2 and C_2, and the equivalent circuit simplified as shown in Fig. 5B. For simplification in the figure, R_{sample} and C_{holder} are expressed as R_1 and C_1, respectively. The impedance of the equivalent circuit is expressed as

$$Z = \frac{R_1 + R_2 + j\omega R_1 R_2 C_2}{1 - \omega^2 R_1 R_2 C_1 C_2 + j\omega(R_1 C_1 + R_2 C_1 + R_2 C_2)}. \quad (1)$$

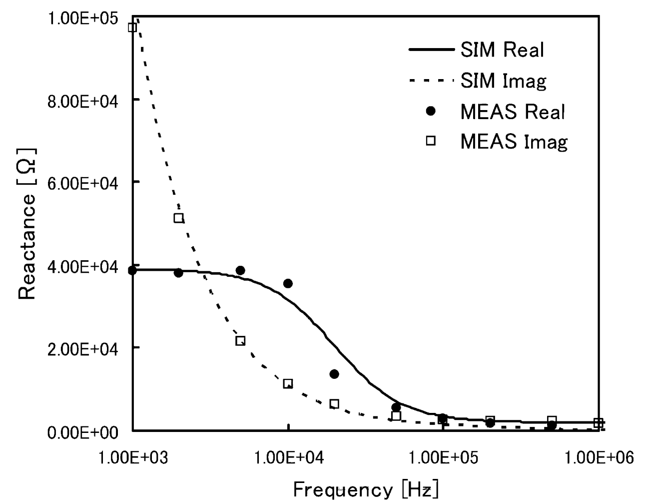

Fig. 6. Plot of the impedance of the sample vs AC bias frequency. The former was expressed as the parallel connection of real and imaginary components at the frequency. The solid circles and open squares show the real and imaginary, respectively, components of the sample measured by the impedance analyzer. The simulated values of the real and imaginary components using the equivalent circuit of the sample and sample holder (see Fig. 5) are plotted in solid and dotted line, respectively.

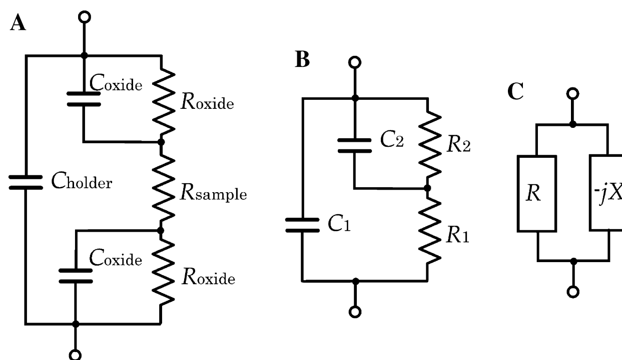

Fig. 5. Equivalent circuits of the sample and sample holder. R_{oxide} and R_{sample} correspond to the resistance of the oxidized layer and the sample material, respectively, C_{holder} to total capacitance of the holder and cable, and C_{oxide} to the capacitance of the oxide layer of the sample (A). The impedances of the oxide layers on both sides of the sample are combined into R_2 and C_2, and to simplify the circuit R_{sample} and C_{holder} are expressed as R_1 and C_1, respectively (B). Because the circuit is composed of resistors and capacitors, the impedance can be expressed as a parallel connection of real and imaginary components (C).

Because the circuit is composed of resistors and capacitors, the impedance can be converted into a parallel connection of real and imaginary components as shown in Fig. 5C, where Z is the impedance of the sample, ω is the angular velocity, and j is the imaginary operator. The real component is expressed as

$$R = \frac{(R_1 + R_2)^2 + \omega^2 R_1^2 R_2^2 C_2^2}{R_1 + R_2 + \omega R_1 R_2^2 C_2^2}, \quad (2)$$

and the imaginary component by

$$-jX = -j\frac{(R_1 + R_2)^2 + \omega^2 R_1^2 R_2^2 C_2^2}{\omega^3 R_1^2 R_2^2 C_1 C_2^2 + \omega R_2^2 C_2 + \omega C_1 (R_1 + R_2)^2}. \quad (3)$$

Using these equations, the values calculated for real and imaginary components are plotted in Fig. 6 in solid and dotted lines, respectively. The value of R_1 was determined by measuring the resistance between the electrodes formed on the other surface of the sample (see Fig. 4B). The resistance of R_2 was the measured real component of the sample at a low frequency. The capacitance of C_1 was determined by measuring the capacitance of an empty sample holder and that of C_2 to fit the calculated and measured values. C_1 and C_2 are negligible at low frequencies and $R_2 \gg R_1$; therefore, the current is almost completely a function of R_2. As the frequency increases, the current begins to flow through C_2, i.e., R_2 is bypassed. Consequently, the contribution of R_1, the resistance of the sample material, to the total impedance gradually increases. However, at higher frequencies, C_1 short circuits (including R_1). Thus, the optimum frequency to observe the change in resistance of the sample material, R_1, might exist between 10 and 100 kHz, where the real component is approximated by R_1 and the imaginary component (approximated to be $1/j\omega C_1$) is large enough so as not to short R_1. Because the AC bias frequency is sufficiently higher than the field modulation frequency (362 Hz), it is possible to detect the EDMR signal, which is synchronized with the field modulation frequency, from the output of the lock-in amplifier for AC bias frequency detection.

3.2. EDMR measurements

Separate EDMR measurements were performed: (a) using a conventional DC bias technique, with metal electrodes formed on the sample surface, as shown in Fig. 4B; (b) using the AC bias technique for the sample, with metal electrodes formed on the sample (Fig. 4B); and (c)

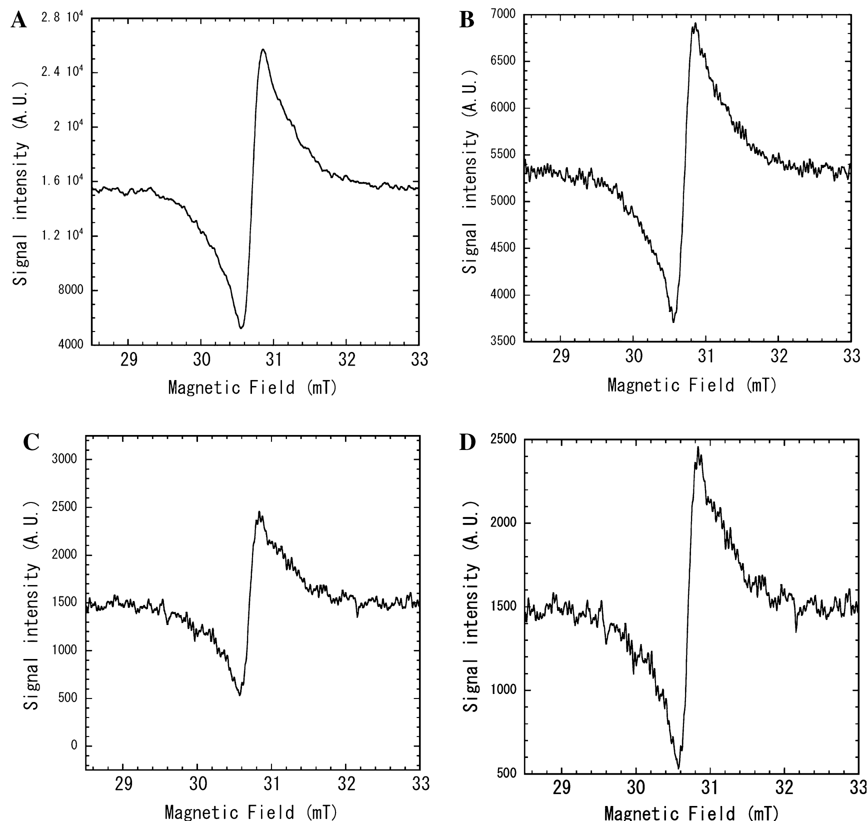

Fig. 7. EDMR spectra: (A) using a conventional DC bias technique for the sample, with metal electrodes formed on the sample surface; (B) using the AC bias technique for the sample with metal electrodes formed on the sample; (C) using the AC bias detection technique for the sample without metal electrodes formed on the sample (instead, using conductive rubber contacts); and (D) an expanded spectrum of (C), the intensity of which was normalized to (A).

using the AC bias technique for the sample but without metal electrodes formed on the sample (instead, using conductive rubber contacts as shown in Fig. 4C). For (a) and (b), the surface of the sample where electrodes were not constructed was illuminated. For (c), the sample was turned inside out when the formed electrodes were not used. The AC bias frequency was set at 10 kHz; and it was possible to observe EDMR signals from 5 to 100 kHz in the AC bias frequencies. The signal intensity was at a maximum around 10 kHz. The noise level was reduced by 30% when a dummy resistor, which was put close to the detection circuit, was substituted. External noise was possibly introduced to the sample and the signal line via stray capacitance. The spectra for all conditions are shown in Figs. 7A–C. SNR for the sample with the AC bias technique was 30% of that obtained by the DC bias technique using electrodes formed on the sample. Signal intensity decreased to 60% when the conductive rubber contacts were used because the additional impedance of the oxide layer reduced the signal intensity. Therefore, total SNR by the AC bias technique was 20% of the value obtained when the DC bias technique was used. An expanded spectrum of Fig. 7C, the intensity of which was normalized to that shown in Fig. 7A, appears in Fig. 7D. The *g*-value, linewidth, and the shape of the spectrum were exactly the same as those obtained when the DC bias technique was employed.

4. Conclusion

Using an AC bias method, non-destructive EDMR measurements of part of a silicon wafer were realized. The EDMR spectrum obtained was the same as that when using a conventional method (i.e., DC bias). SNR was worse when AC bias was used; however, because the noise appeared to be coming from outside, ample room exists to improve the sensitivity of the AC bias technique. This AC bias technique can be applied to measure various bulk materials; in addition, it should be applicable to systems in which oxidization or reduction caused by a DC bias current corrupts the system.

Acknowledgments

We thank Dr. T. Mineta of Hirosaki University and Mr. Z. Watanabe of Yamagata Research Institute of Technology for their helpful discussions and assistance in manufacturing silicon samples with electrodes. This research was supported by a Grant-in-Aid for Scientific Research (15350051) from the Ministry of Education, Culture, Sports, Science and Technology of Japan.

References

[1] D.J. Lepine, Spin-dependent recombination on silicon surface, Phys. Rev. B 6 (1972) 436–441.
[2] I. Solomon, Spin-dependent recombination in a silicon *p-n* junction, Solid State Commun. 20 (1976) 215–217.
[3] A. Maier, A. Grupp, M. Mehring, Electrically detected electron spin resonance (EDESR) in Thiophene thin films and a Thiophene/C60 double layer, Solid State Commun. 99 (1996) 623–626.
[4] W.E. Carlos, E.R. Glaser, T.A. Kennedy, S. Nakamura, Paramagnetic resonance in GaN-based light emitting diodes, Appl. Phys. Lett. 67 (1995) 2376–2378.
[5] D. Kaplan, I. Solomon, N.F. Mott, Explanation of the large spin-dependent recombination effect in semiconductors, J. Phys. (Paris) 39 (1978) 51–54.
[6] F.C. Rong, W.R. Buchwald, E.H. Poindexter, W.L. Warren, D.J. Keeble, Spin-dependent Shockley-Read recombination of electrons and holes in indirect-band-gap semiconductor *p-n* junction diodes, Solid State Electron. 34 (1991) 835–841.
[7] I. Solomon, Spin physics in disordered semiconductors, Bull. Magn. Reson. 5 (1983) 118–119.
[8] R.L. Vranch, B. Henderson, M. Pepper, Spin-dependent recombination in irradiated Si/SiO_2 device structures, Appl. Phys. Lett. 52 (1988) 1161–1163.
[9] M.S. Brandt, M.W. Bayerl, N.M. Reinacher, T. Wimbauer, M. Stutzmann, Electrically detected magnetic resonance at different microwave frequencies, Mater. Sci. Forum 258–263 (1997) 963–968.
[10] A.V. Barabanov, V.A. L'vov, O.V. Tretyak, Spin-dependent recombination: influence of weak magnetic fields, in: 23rd International Conference on the Physics of Semiconductors, vol. 4, 1996, pp. 2693–2696.
[11] T. Sato, H. Yokoyama, H. Ohya, H. Kamada, Electrically detected magnetic resonance signal intensity at resonant frequencies from 300 to 900 MHz in a constant microwave field, J. Magn. Reson. 139 (1999) 422–429.
[12] K. Fukui, T. Sato, H. Yokoyama, H. Ohya, H. Kamada, Resonance-field dependence in electrically detected magnetic resonance: effect of exchange interaction, J. Magn. Reson. 149 (2001) 13–21.
[13] T. Sato, H. Yokoyama, H. Ohya, H. Kamada, Development and evaluation of L-band electrically detected magnetic resonance (EDMR) spectrometer operating at 900 MHz, Rev. Sci. Instrum. 71 (2000) 486–493.
[14] T. Sato, H. Yokoyama, H. Ohya, H. Kamada, Imaging of electrically detected magnetic resonance of a silicon wafer, J. Magn. Reson. 153 (2001) 113–116.
[15] T. Sato, H. Yokoyama, H. Ohya, H. Kamada, Visualizing an artificial recombination pattern formed by localized illumination in a semiconductor, Chem. Lett. 33 (2004) 650–651.
[16] M. Ono, T. Ogata, K. Hsieh, M. Suzuki, E. Yoshida, H. Kamada, L-band ESR spectrometer using a loop-gap resonator for in-vivo analysis, Chem. Lett. (1986) 491–494.
[17] H. Hirata, H. Iwai, M. Ono, Resonance frequency estimation of a bridged loop-gap resonator used for magnetic resonance measurements, Rev. Sci. Instrum. 67 (1996) 73–78.